Available online at www.sciencedirect.com

ScienceDirect

Current Opinion in Electrochemistry

Review Article

# Measurement and interpretation of the double layer capacitance of Pt(111)/aqueous solution interfaces

Lulu Zhang[1] and Jun Huang[1,2]

**Abstract**

The electric double layer (EDL) at Pt(111)/aqueous solution interfaces is, in some sense, a shelter for electrocatalysis, where one can find solace in exploring the fundamentals before venturing into the labyrinthine landscape of real-world intricacies. Although seemingly unpretentious, classical electrochemical methods such as cyclic voltammetry (CV) and electrochemical impedance spectroscopy (EIS) play an indispensable role in quantitative investigation of this EDL. However, these measurements and interpretation are highly nontrivial, and three related issues are addressed in this Opinion article. First, we discuss discrepancies among various measurements of the double layer capacitance $C_{dl}$, and recommend separating $C_{dl}$ from possible pseudo-capacitances using EIS. Second, following our recommendation, we examine assumptions and limitations of the Frumkin–Melik–Gaikazyan (FMG) model that is *the* physical model used to extract $C_{dl}$ from EIS data in the presence of chemisorption. Thirdly, we compare CV-derived $C_{dl}$ and EIS-derived $C_{dl}$. We explain why EIS-derived $C_{dl}$ is always positive even for the case where CV-derived $C_{dl}$ assumes negative values due to partially charged adsorbates. We hope this Opinion can facilitate the advent of a converged understanding of the EDL at Pt(111)/aqueous solution interfaces.

**Addresses**

[1] Institute of Energy and Climate Research, IEK-13: Theory and Computation of Energy Materials, Forschungszentrum Jülich GmbH, 52425 Jülich, Germany

[2] Theory of Electrocatalytic Interfaces, Faculty of Georesources and Materials Engineering, RWTH Aachen University, 52062 Aachen, Germany

Corresponding author: Huang, Jun (ju.huang@fz-juelich.de)

**Current Opinion in Electrochemistry** 2023, **42**:101419

This review comes from a themed issue on **Fundamental and Theoretical Electrochemistry (2024)**

Edited by **Kai S. Exner**

For complete overview about the section, refer Fundamental and Theoretical Electrochemistry (2024)

Available online 2 November 2023

**https://doi.org/10.1016/j.coelec.2023.101419**



**Keywords**

Electric double layer, Double layer capacitance, Adsorption impedance, Negative capacitance, Pt(111)/aqueous solution interfaces.

## Measurements of $C_{dl}$

In stark contract with minor fluctuations among the cyclic voltammograms (CV) of Pt(111) in 0.1 M $HClO_4$ electrolyte solution as documented in previous studies [1–4], the measurements of double layer capacitance ($C_{dl}$) of Pt(111) in similar electrolyte solutions exhibit substantial divergence. This significant discrepancy poses a critical challenge for evaluating the effectiveness of existing double layer models pertaining to these interfaces.

Figure 1(a) displays four CVs in terms of capacitance obtained by dividing the current density by the scanning rate. Small peaks in the hydrogen adsorption/desorption region between 0.05 $V_{RHE}$ and around 0.4 $V_{RHE}$ are usually attributed to defects on Pt(111), see a recent Opinion [5]. The butterfly peak between 0.55 $V_{RHE}$ and 0.9 $V_{RHE}$ corresponds to hydroxyl adsorption/desorption [6–8]. The butterfly consists of a prewave and a sharp peak. It is generally accepted that the prewave corresponds to long-range disordered adsorption, and the sharp peak corresponds to phase transition to long-range ordered adsorption [9]. This butterfly peak is incompletely understood, as evidenced by unexpected influence of perchlorate anions on the butterfly [10–12].

The nearly flat, low-lying region from 0.4 $V_{RHE}$ to 0.55 $V_{RHE}$ is assumed to be a pure double layer charging region [8]. Figure 1(b) zooms into this region of Figure 1(a). A variation on the magnitude of 40 $\mu F/cm^{-2}$ is observed. Moreover, a common capacitance minimum is found at 0.50 $V_{RHE}$. This capacitance minimum is unlikely the Gouy-Chapman minimum [13] since the potential of zero charge (PZC) of Pt(111) in 0.1 M $HClO_4$ is around 0.35 $V_{RHE}$ [14,15]. Instead, the capacitance minimum is likely resulted from the transition from the decreasing pseudo-capacitance of hydrogen desorption to the increasing pseudo-capacitance of hydroxyl adsorption as the potential

**Figure 1**

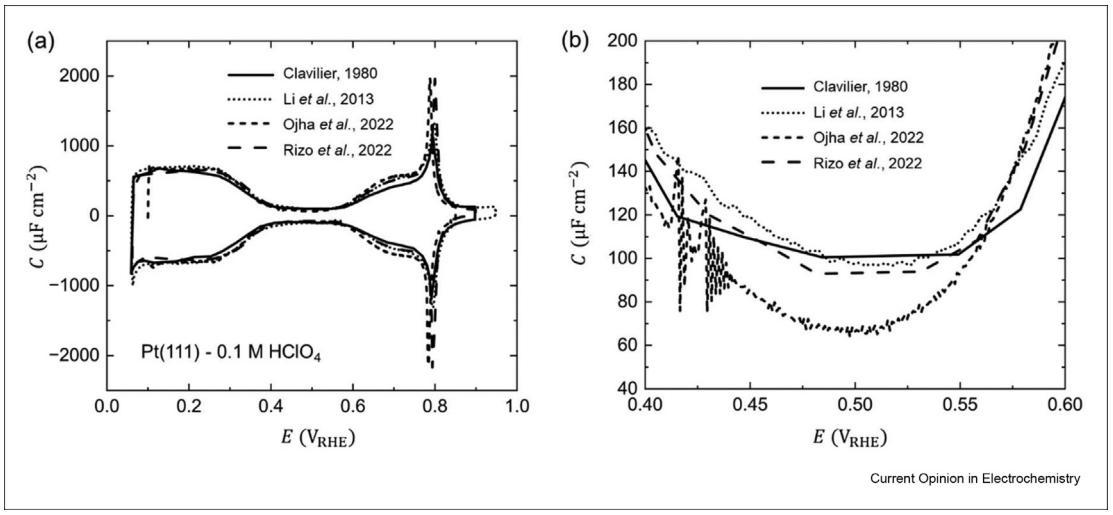


(**a**) Comparison between cyclic voltammograms of Pt(111)-0.1 M $HClO_4$ solution interfaces from Clavilier [3] (solid line), Li et al. [4] (short dot line), Ojha et al. [1] (short dash line), and Rizo et al. [2] (dash line). (**b**) An enlarged view of Figure 1(a) in the double layer region from 0.4 $V_{RHE}$ to 0.6 $V_{RHE}$.

shifts positive [16]. Shifting the PZC to around 0.5 $V_{RHE}$ requires a solution pH of around 3.

Figure 2(a) shows three curves of the double layer capacitances ($C_{dl}$) in less acidic media measured by three groups using different methods [1,17,18]. No similarity can be found between these results. The earlier $C_{dl}$ from Pajkossy and Kolb has an "S" shape, constituting of an initial decrease up to 0.35 $V_{RHE}$, an increase till 0.6 $V_{RHE}$ and then a decreasing trend. The recent $C_{dl}$ from Garlyyev et al. is "U" shaped with a low-lying plateau from 0.3 $V_{RHE}$ to 0.45 $V_{RHE}$. In contrary, a "W"-shaped $C_{dl}$ profile was obtained by Ojha et al. more recently. At such low concentrations of the electrolyte solution, the classical Gouy-Chapman-Stern (GCS) model predicts a camel-shaped $C_{dl}$ profile with the minimum pinpointed at the PZC [13,19]. The deviation from the GCS model has triggered the development of several models for this

**Figure 2**

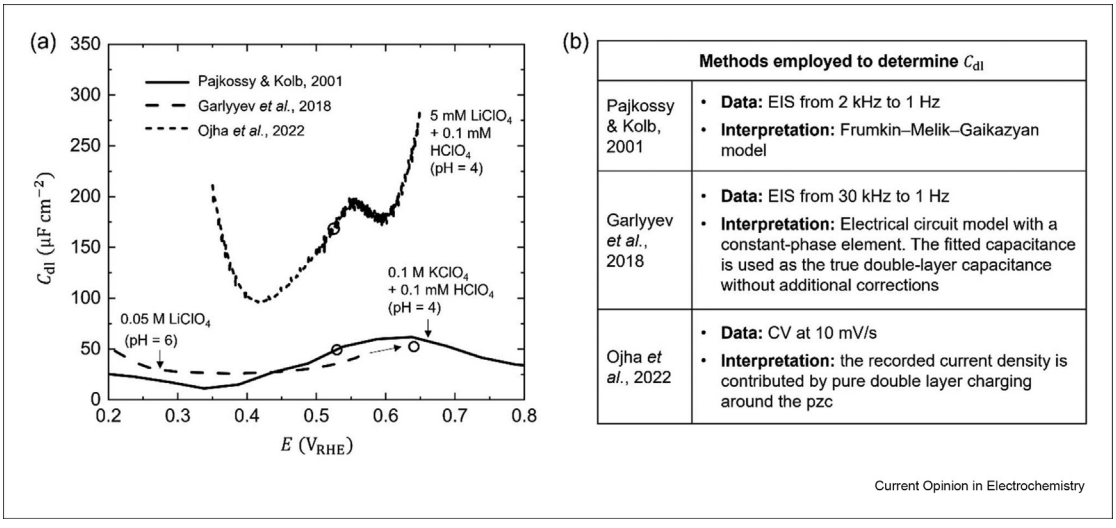


(**a**) Comparison between double layer capacitances ($C_{dl}$) of Pt(111)/aqueous solution interfaces from Pajkossy and Kolb [17] (solid line), Garlyyev et al. [18] (dash line) and Ojha et al. [1] (short dash line). The PZC for each system is calculated by 0.29 + 0.059 pH $V_{RHE}$, and denoted by the cycles. More details of the methods of determining $C_{dl}$ are listed in (**b**).

EDL, which has been critically reviewed in a recent Opinion [20].

In addition to variations in shape, the magnitude of $C_{dl}$ also exhibits divergence. According to the GCS model, $C_{dl}$ should decrease in more diluted solutions at the same electrode potential relative to the PZC [13]. However, the experimental data from three different studies do not conform to this theory. The data of Pajkossy and Kolb [17] were obtained in 0.1 M $KClO_4$ and 0.1 mM $HClO_4$ solution at pH 4, ranging from 10 to 60 $\mu F/cm^2$ as $E$ varies between 0.2 $V_{RHE}$ and 0.8 $V_{RHE}$. Ojha et al. [1] measured $C_{dl}$ in 5 mM $LiClO_4$ + 0.1 mM $HClO_4$ with the lowest concentration among the three experiments, is, nevertheless, the highest, ranging from 100 to 300 $\mu F/cm^2$ as $E$ varies between 0.35 $V_{RHE}$ and 0.65 $V_{RHE}$.

As pointed out recently [16], the discrepancies in shape and magnitude of the $C_{dl}$ profiles could be traced back to different methods employed to determine $C_{dl}$, in addition to inevitable differences in the cleanness of the electrolyte solution. Pajkossy and Kolb extracted $C_{dl}$ from electrochemical impedance spectroscopy (EIS) data in a frequency range of 2 kHz to 1 Hz. The Frumkin–Melik–Gaikazyan (FMG) model was used to separate $C_{dl}$ from the adsorption capacitance $C_{ad}$ [17]. Garlyyev et al. extracted $C_{dl}$ from EIS data in a frequency range of 30 kHz to 1 Hz using an electrical circuit model with a constant-phase element (CPE) [18]. The exponent coefficient $n$ in the CPE is found to be $n = 0.96 \pm 0.01$. Therefore, the fitted capacitance was approximated as the true double-layer capacitance without additional corrections. The $C_{dl}$ from Ojha et al. was calculated from current density recorded in CV measurements. With a deliberate choice of the solution pH in the range between 3 and 4, the PZC falls into the double layer region. They assumed that the recorded current density is contributed solely by pure double layer charging, and the total converted capacitance is believed to be equivalent to $C_{dl}$ [1].

In principle, EIS can separate $C_{dl}$ from possible pseudo-capacitances of chemisorption, rendering it the method of choice for $C_{dl}$ measurements [21,22]. The total capacitance $C_{total}$ is reduced to $C_{dl}$ only when the frequency is above a characteristic frequency $\omega_c$ based on the FMG model, as to be analyzed in the following section. At low frequencies, one will find $C_{total}(\omega \to 0) \approx C_{dl} + C_{ad}$, where $C_{ad}$ is the adsorption capacitance. The characteristic frequency $\omega_c$ is around 1 MHz for hydrogen adsorption at Pt(111) in 0.5 M perchloric acid [23], and above 10 kHz for hydroxyl adsorption at Pt(111) in 0.1 M perchloric acid [24]. A scanning rate of 10 mV $s^{-1}$ corresponds to a characteristic frequency below 1 Hz, which is far lower than the typical $\omega_c$ of Pt(111) electrode processes. Therefore, it is extremely difficult to separate $C_{dl}$ from $C_{ad}$, if any, in CV measurements.

Albeit being a routine classical electrochemical experiment, accurate measurement of the $C_{dl}$ of Pt/aqueous solution interfaces presents a considerable challenge. As is well known, this is mainly due to the high sensitivity of this interface to minute impurities in the electrolyte solution and a tiny portion of defects on the metal surface. Compared to the linear scanning voltammetry, the alternating cyclic voltammetry seems to better serve the purpose for it allows to filter slow adsorption processes by selecting the frequency [25]. However, it is crucial to establish that the $C_{dl}$ does not change significantly with the applied frequency, as demonstrated in Valette's measurements on silver [26]. Given the likely presence of fast chemisorption processes, we recommend determining $C_{dl}$ from EIS measurements and using a physical model to extract $C_{dl}$. As emphasized in the last section, $C_{dl}$ obtained this way corresponds to a very high frequency. EIS measurements on electrocatalytic interfaces are highly nontrivial. In EIS measurements, it is highly important to be aware of high-frequency artefacts brought by the reference electrode and the measurement system, as elaborated by Tran et al. [27], and to understand the assumptions and limitations of the prevailing physical model – the FMG model, which are discussed below [22].

## Extraction of $C_{dl}$ from EIS using Frumkin–Melik–Gaikazyan model

If one employs EIS to determine $C_{dl}$, a proper model is required to extract $C_{dl}$ from the measured EIS data. The appropriateness of the model determines the reliability of the extracted $C_{dl}$. Therefore, it is crucial to understand the assumptions and limitations of the model used in data analysis.

The FMG model is the physical model for electrocatalytic EDLs with chemisorption [28,29]. The illustration and corresponding FMG model of EDL are shown in Figure 3(a) and (b) [22]. The FMG model describes the chemisorption process using a charge transfer resistance $R_{ad}$, a pseudo-capacitance of chemisorption $C_{ad}$, and a diffusion impedance $W$, which are in series. The double layer capacitance $C_{dl}$ is in parallel connection with the chemisorption branch. In addition, the resistance of the bulk solution $R_s$ is used to describe the ionic conduction in the electrolyte solution. The total capacitance expressed by the FMG model reads,

$$C(\omega) = \frac{1}{j\omega(Z - R_s)} = C_{dl} + \frac{C_{ad}}{j\omega C_{ad}(R_{ad} + W) + 1} \qquad (1)$$

where $Z$ is the total interfacial impedance, $\omega$ the angular frequency. The diffusion impedance $W$ is often described by the Warburg formula, $W = \sigma_D(j\omega)^{-0.5}$ with $\sigma_D$ being a coefficient as a function of the diffusion coefficient [30].

**Figure 3**

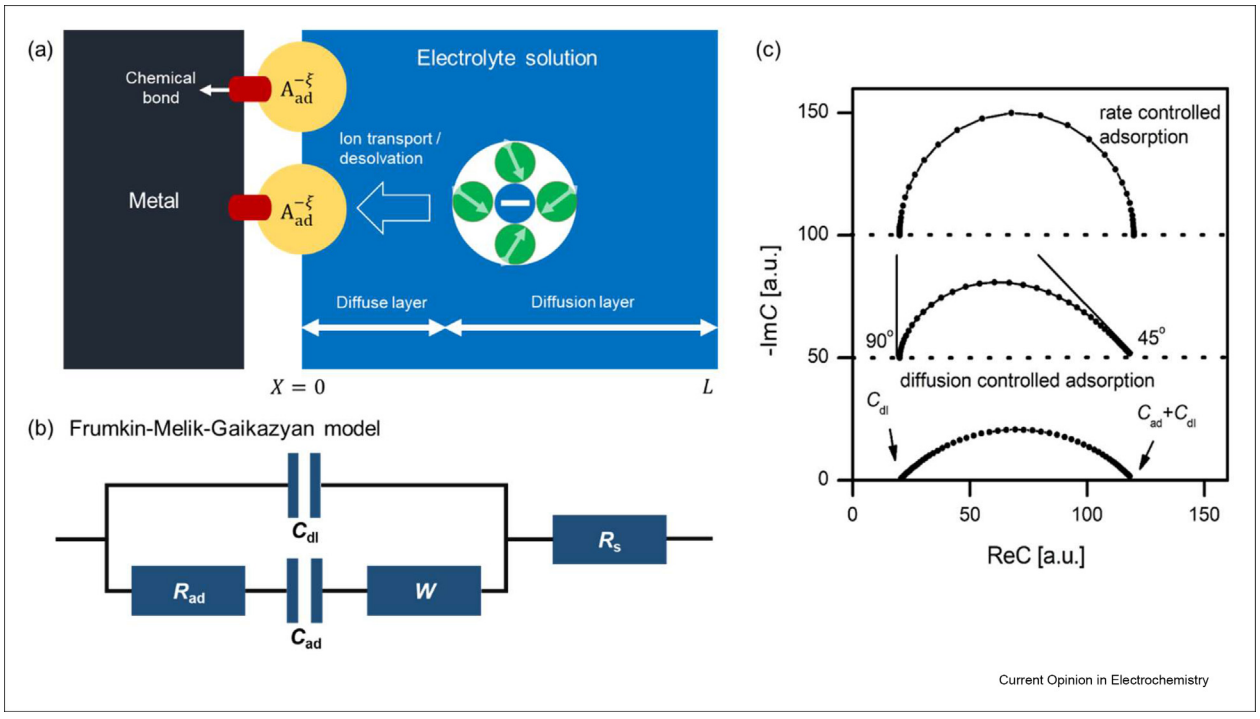


(**a**) The Schematic illustration and (**b**) the corresponding FMG model describing the electrocatalytic EDL with chemisorption [22]. (**c**) The capacitance spectra at slow, medium and fast rates of chemisorption, reproduced with permission from Ref. [17]. Copyright, Elsevier.

Figure 3(c) shows the capacitance spectra at slow, medium and fast rates of chemisorption, with the frequency decreasing clockwise [17]. $C(\omega)$ is asymptotic to $C_{dl}$ as $\omega \to \infty$, and to $C_{dl} + C_{ad}$ as $\omega \to 0$ according to Eq. (1). In the intermediate frequency range, $C(\omega)$ is manifested as an arc which becomes more squashed as the diffusion impedance plays a more important role [17,29,31].

The FMG model has several limitations [22]. First, the EDL charging process and the electron transfer process are decoupled, described by $C_{dl}$ and $R_{ad}$, respectively. In reality, electron transfer reactions and EDL charging are intrinsically coupled, which not only impacts the magnitude but also changes the shape of EIS. In a recent work, an inductive loop in low frequency range is ascribed to the aforementioned coupling under nonequilibrium states [32]. Second, both the EDL charging process ($C_{dl}$) and the mass transport process ($R_s$) belong to ion transport in the electrolyte solution but are separately described in the FMG model. Third, $C_{dl}$ is taken as a frequency-independent constant, which is problematic as the EDL charging is an ion transport process which should manifest frequency dispersion [29,33]. At last, the ion transport process is described using the Warburg formula which is limited to pure Fickian diffusion in semi-infinite, dilute electrolyte solution [34]. These limitations have been addressed in an improved model developed by Huang and Li [22].

## Comparison of $C_{dl}$ obtained from EIS and surface free charge density

The above discussion revolves around two different kinds of $C_{dl}$, including $C_{dl}$ determined from EIS, denoted $C_{dl}^{EIS}$, and that from CV, or equivalently, the surface free charge density $\sigma_{free}$, $C_{dl}^{\sigma} = \frac{\partial \sigma_{free}}{\partial E}$ [16]. Table 1 compares the two methods. A striking difference is that while $C_{dl}^{EIS}$ is always positive, $C_{dl}^{\sigma}$ can be negative in the presence of partially negatively charged adsorbed intermediates [16,35].

The difference between $C_{dl}^{EIS}$ and $C_{dl}^{\sigma}$ is due to the hidden fact that they correspond to disparate different frequencies. $C_{dl}^{\sigma}$ obtained from the equilibrium surface charging relation corresponds to a zero frequency. However, when trying to separate $C_{dl}$ from $C_{ad}$ using the FMG model, we actually go to extremely high frequency such that the adsorption and desorption cannot follow up the rapid potential change and do not contribute to the current signal. In this scenario, the origin of negative $C_{dl}$, namely, the change in the chemisorption-induced surface dipoles, is absent at such high frequencies. Therefore, $C_{dl}^{EIS}$ is always positive because it is a structural capacitance. It is worth noting that the frequency

**Table 1**

**Comparison of $C_{dl}$ obtained from two methods.**

| Data | EIS | Surface free charge density or CV (if there is no chemisorption) |
|---|---|---|
| Method | Fitting EIS data using Eq. (1) | $C_{dl} = \frac{\partial \sigma_{free}}{\partial E}$ |
| Frequency | High enough so that chemisorption does not occur | Zero |
| Property | Always positive | Could be negative due to adsorbed intermediates with partial negative charge |

embedded in $C_{dl}^{EIS}$ is not infinitely high, otherwise even ions cannot move and the resultant $C_{dl}^{EIS}(\omega \to \infty)$ is a pure structural capacitance [36].

Now, we take the Pt(111)-$HClO_4$ interface as an example to further show the difference between $C_{dl}^{EIS}$ and $C_{dl}^{\sigma}$. Utilizing the EDL model depicted in Figure 4(a) [16], we calculate both $C_{dl}^{EIS}$ and $C_{dl}^{\sigma}$, with details provided in the supporting information. We assume that adsorbed ions $A_{ad}$ have a negative charge of $-0.1\ e_0$ and its coverage $\theta_A$ increases with the electrode potential as shown in Figure 4(c). The negative charge carried by $A_{ad}$ turns $\sigma_{free}$ toward more negative values as the coverage increases, leading to negative $C_{dl}^{\sigma}$ until $\theta_A$ reaches the maximum. Physical origins of this negative $C_{dl}^{\sigma}$ are referred to a previous Opinion [37]. $C_{dl}^{EIS}$ is calculated using the same model but now the adsorption of ions A does not change at such high frequencies, namely, $\theta_A$ is fixed. $C_{dl}^{EIS}$ is always positive and has its minimum at the PZC. Last but not the least, the negative $C_{dl}$ can also be obtained from the impedance model developed by Huang and Li at low frequencies [22], as introduced in the supporting information.

## Conclusion

Three questions pertaining to the Pt(111)/aqueous solution interfaces have been discussed. First, significant discrepancies among different measurements of the double layer capacitance have been observed, which could be attributed to variations in the methodologies used to determine $C_{dl}$. We recommend determining $C_{dl}$ from EIS measurements in conjunction with a physical model to eliminate the influence of unintended fast chemisorption processes. Second, the Frumkin-Melik-Gaikazyan (FMG) model has been analyzed in terms of its assumptions and limitations, compared to a modified model developed by Huang and Li [22]. Lastly, we compare $C_{dl}^{\sigma}$ calculated from the surface free

**Figure 4**

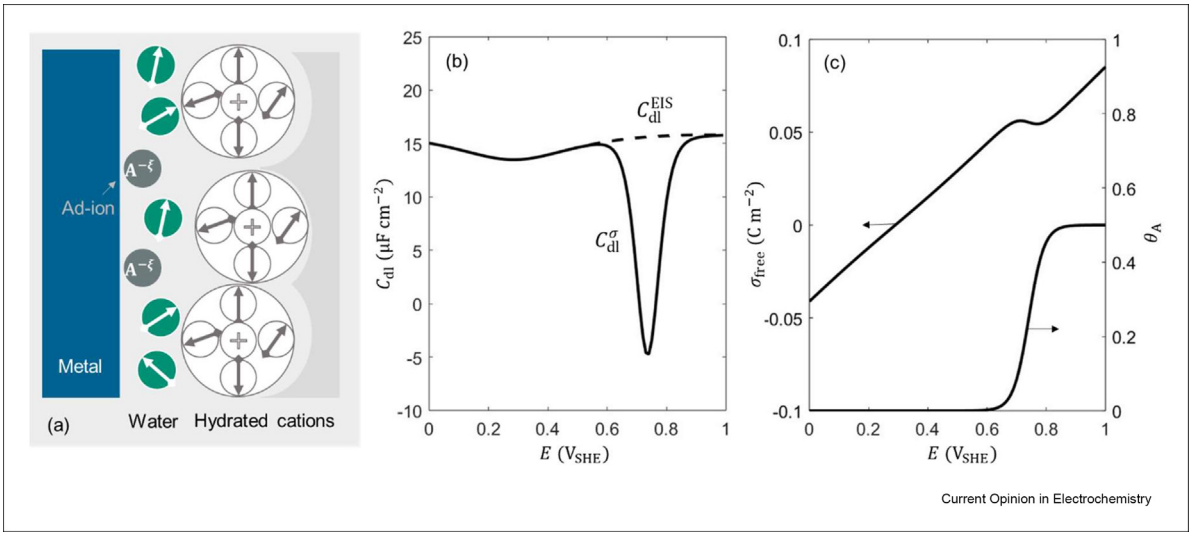


(**a**) The structure of an electrocatalytic EDL with partially charged adsorbates, reproduced with permission from Ref. [16] (**b**) The calculated double layer capacitance determined from EIS, denoted $C_{dl}^{EIS}$, and that from CV, $C_{dl}^{\sigma}$, as well as (**c**) the calculated surface free charge density, $\sigma_{free}$, and the coverage of adsorbed A, $\theta_A$, as a function of the electrode electric potential for the Pt(111)-$HClO_4$ interface. Model parameters are listed in the supporting information of this article.

charge density and $C_{dl}^{EIS}$ extracted from EIS data in conjunction of a proper model. $C_{dl}^{EIS}$ is always positive, while $C_{dl}^{\sigma}$ could be negative in the presence of negatively charged adsorbates. This discrepancy arises because the latter is obtained only at high frequencies, while the former is an equilibrium quantity that corresponds to a zero frequency. The negative $C_{dl}$ can be inferred from nontraditional measurements of surface charge, e.g., via the laser-induced temperature jump method [14,38].

## Declaration of competing interest

The authors declare the following financial interests/personal relationships which may be considered as potential competing interests: Jun Huang reports financial support was provided by Helmholtz Association of German Research Centres.

## Data availability

Data will be made available on request.

## Acknowledgement

This work is supported by the Initiative and Networking Fund of the Helmholtz Association (No. VH-NG-1709). We appreciate Dr. Tamas Pajkossy for providing original data in Ref. [17].

## Appendix A. Supplementary data

Supplementary data to this article can be found online at https://doi.org/10.1016/j.coelec.2023.101419.

## References

Papers of particular interest, published within the period of review, have been highlighted as:

* of special interest
** of outstanding interest

1. * Ojha K, Doblhoff-Dier K, Koper MTM: **Double-layer structure of the pt(111)–aqueous electrolyte interface**. *Proc Natl Acad Sci USA* 2022, **119**, e2116016119.
New data and a new model of the EDL at Pt(111)/aqueous solution interface.

2. * Rizo R, Fernández-Vidal J, Hardwick LJ, Attard GA, Vidal-Iglesias FJ, Climent V, Herrero E, Feliu JM: **Investigating the presence of adsorbed species on pt steps at low potentials**. *Nat Commun* 2022, **13**:2550.
State-of-the-art cyclic voltammograms and understanding of Pt single crystal electrodes.

3. Clavilier J: **The role of anion on the electrochemical behaviour of a {111} platinum surface; an unusual splitting of the voltammogram in the hydrogen region**. *J Electroanal Chem Interfacial Electrochem* 1980, **107**:211–216.

4. Li MF, Liao LW, Yuan DF, Mei D, Chen YX: **Ph effect on oxygen reduction reaction at pt(111) electrode**. *Electrochim Acta* 2013, **110**:780–789.

5. Rizo R, Herrero E, Climent V, Feliu JM: **On the nature of adsorbed species on platinum single-crystal electrodes**. *Curr Opin Electrochem* 2023, **38**, 101240.

6. Hamm UW, Kramer D, Zhai RS, Kolb DM: **The pzc of au(111) and pt(111) in a perchloric acid solution: an ex situ approach to the immersion technique**. *J Electroanal Chem* 1996, **414**:85–89.

7. Climent V, Feliu JM: **Surface electrochemistry with pt single-crystal electrodes**. In *Advances in electrochemical science and engineering*; 2017:1–57.

8. Herrero E, Feliu JM, Wieckowski A, Clavilier J: **The unusual adsorption states of pt(111) electrodes studied by an iodine displacement method: Comparison with au(111) electrodes**. *Surf Sci* 1995, **325**:131–138.

9. Koper MTM, Lukkien JJ: **Modeling the butterfly: the voltammetry of ($\sqrt{3}\times\sqrt{3}$)r30° and p(2×2) overlayers on (111) electrodes**. *J Electroanal Chem* 2000, **485**:161–165.

10. Attard GA, Brew A, Hunter K, Sharman J, Wright E: **Specific adsorption of perchlorate anions on pt{hkl} single crystal electrodes**. *Phys Chem Chem Phys* 2014, **16**:13689–13698.

11. Fröhlich N, Fernández-Vidal J, Mascaró FV, Shih AJ, Luo M, Koper MTM: **Effect of trace impurities in perchloric acid on blank voltammetry of pt(111)**. *Electrochim Acta* 2023, **466**, 143035.

12. Luo M, Koper MTM: **A kinetic descriptor for the electrolyte effect on the oxygen reduction kinetics on pt(111)**. *Nat Catal* 2022, **5**:615–623.

13. López-García JJ, Horno J, Grosse C: **Differential capacitance of the diffuse double layer at electrode-electrolyte interfaces considering ions as dielectric spheres: Part i. Binary electrolyte solutions**. *J Colloid Interface Sci* 2017, **496**:531–539.

14. ** Sebastián P, Martínez-Hincapié R, Climent V, Feliu JM: **Study of the pt (111) | electrolyte interface in the region close to neutral ph solutions by the laser induced temperature jump technique**. *Electrochim Acta* 2017, **228**:667–676.
Important insights into the EDLs at Pt(111)/aqueous solution interface from laser induced temperature jump experiments.

15. Martínez-Hincapié R, Climent V, Feliu JM: **Peroxodisulfate reduction as a probe to interfacial charge**. *Electrochem Commun* 2018, **88**:43–46.

16. ** Huang J: **Zooming into the inner helmholtz plane of pt(111)–aqueous solution interfaces: chemisorbed water and partially charged ions**. *Journal of the American Chemical Society Au* 2023, **3**:550–564.
Alternative explanation of the double-layer capacitance derived from cyclic voltammograms.

17. Pajkossy T, Kolb DM: **Double layer capacitance of pt(111) single crystal electrodes**. *Electrochim Acta* 2001, **46**:3063–3071.

18. Garlyyev B, Xue S, Watzele S, Scieszka D, Bandarenka AS: **Influence of the nature of the alkali metal cations on the electrical double-layer capacitance of model pt(111) and au(111) electrodes**. *J Phys Chem Lett* 2018, **9**:1927–1930.

19. Zhang LL, Li CK, Huang J: **A beginners guide to modelling of electric double layer under equilibrium, nonequilibrium and ac conditions**. *Journal of Electrochemistry* 2022, **28**, 2108471.

20. ** Doblhoff-Dier K, Koper MTM: **Electric double layer of pt(111): known unknowns and unknown knowns**. *Curr Opin Electrochem* 2023, **39**, 101258.
A comparative analysis of three models for Pt(111)/aqueous solution interface.

21. Sluyters-Rehbach M: **Impedances of electrochemical systems: terminology, nomenclature and representation - part i: cells with metal electrodes and liquid solutions (iupac recommendations 1994)**. *Pure Appl Chem* 1994, **66**:1831–1891.

22. Huang J, Li CK: **Impedance response of electrochemical interfaces: Part ii-chemisorption**. *J Phys Condens Matter* 2021, **33**, 164003.

23. Sibert E, Faure R, Durand R: **High frequency impedance measurements on pt(111) in sulphuric and perchloric acids**. *J Electroanal Chem* 2001, **515**:71–81.

24. Schouten KJP, van der Niet MJTC, Koper MTM: **Impedance spectroscopy of h and oh adsorption on stepped single-crystal platinum electrodes in alkaline and acidic media**. *Phys Chem Chem Phys* 2010, **12**:15217–15224.

25. Fawcett WR, Kováčová Z, Motheo AJ, Foss CA: **Application of the ac admittance technique to double-layer studies on polycrystalline gold electrodes**. *J Electroanal Chem* 1992, **326**:91–103.

26. Valette G: **Double layer on silver single-crystal electrodes in contact with electrolytes having anions which present a slight specific adsorption: Part i. The (110) face**. *J Electroanal Chem Interfacial Electrochem* 1981, **122**:285–297.

27. Tran AT, Huet F, Ngo K, Rousseau P: **Artefacts in electrochemical impedance measurement in electrolytic solutions due to the reference electrode**. *Electrochim Acta* 2011, **56**: 8034–8039.

28. Frumkin A, Melik-Gaikazyan: *Determination of the kinetics of adsorption of organic substances by measurements of the differential capacity and the conductance of the boundary between electrodes and solutions*. 1951.

29. Huang J: **Electrochemical impedance spectroscopy for electrocatalytic interfaces and reactions: classics never die**. *Journal of Electrochemistry* 2020, **26**:3–18.

30. Warburg E: **Ueber das verhalten sogenannter unpolarisirbarer elektroden gegen wechselstrom**. *Ann Phys* 1899, **303**: 493–499.

31. Li CK, Huang J: **Impedance response of electrochemical interfaces: Part i. Exact analytical expressions for ideally polarizable electrodes**. *J Electrochem Soc* 2020, **167**, 166517.

32. Li CK, Zhang J, Huang J: **Impedance response of electrochemical interfaces. Iii. Fingerprints of couplings between interfacial electron transfer reaction and electrolyte-phase ion transport**. *J Chem Phys* 2022, **157**, 184704.

33. Robertson WD: **The capacity of polarized platinum electrodes in hydrochloric acid**. *J Electrochem Soc* 1953, **100**:194–201.

34. Huang J: **Diffusion impedance of electroactive materials, electrolytic solutions and porous electrodes: Warburg impedance and beyond**. *Electrochim Acta* 2018, **281**:170–188.

35. Huang J, Malek A, Zhang J, Eikerling MH: **Non-monotonic surface charging behavior of platinum: a paradigm change**. *J Phys Chem C* 2016, **120**:13587–13595.

36. Zhang Z, Li C, Zhang J, Eikerling M, Huang J: **Dynamic response of ion transport in nanoconfined electrolytes**. *Nano Lett* 2023, https://doi.org/10.1021/acs.nanolett.3c02560.

37. * Huang J: **Surface charging behaviors of electrocatalytic interfaces with partially charged chemisorbates**. *Curr Opin Electrochem* 2022, **33**, 100938.
A minireview on how partially charged chemisorbates change the double layer, especially, the surface charging behavior.

38. Climent V, Coles BA, Compton RG: **Coulostatic potential transients induced by laser heating of a pt(111) single-crystal electrode in aqueous acid solutions. Rate of hydrogen adsorption and potential of maximum entropy**. *J Phys Chem B* 2002, **106**:5988–5996.